ELSEVIER

Polymer 43 (2002) 4879–4886

polymer

www.elsevier.com/locate/polymer

The atactic polystyrene molecular weight effect on the thermal properties and crystal structure of syndiotactic polystyrene/atactic polystyrene blends

Fang-Chyou Chiu*, Chi-Gong Peng

Department of Chemical and Materials Engineering, Chang Gung University, Tao-Yuan 333, Taiwan, ROC

Received 18 February 2002; received in revised form 20 May 2002; accepted 22 May 2002

Abstract

This work examined how the molecular weight of atactic polystyrene (aPS) affects the thermal properties and crystal structure of syndiotactic polystyrene (sPS)/aPS blends using differential scanning calorimetry, polarized light microscopy and wide angle X-ray diffraction (WAXD) technique. For comparative purposes, the structure and properties of the parent sPS was also investigated. The experimental results indicated that these blends showed single glass transition temperatures (T_gs), implying the miscibility of these blends in the amorphous state regardless of the aPS molecular weight. The non-isothermal and isothermal melt crystallization of sPS were hindered with the incorporation of aPSs. Moreover, aPS with a lower molecular weight caused a further decrease in the crystallization rate of sPS. Complex melting behavior was observed for parent sPS and its blends as well. The melting temperatures of these blends were lower than those of the parent sPS, and they decreased as the molecular weight of aPS decreased. Compared with the results of the WAXD study, the observed complex melting behavior resulted from the mixed polymorphs (i.e. the α and β forms) along with the melting–recrystallization–remelting of the β form crystals during the heating scans. The degree of melting–recrystallization–remelting phenomenon for each specimen was dependent primarily on how fast the sPS crystals were formed instead of the incorporation of aPSs. Furthermore, the existence of aPS in the blends, especially the lower molecular weight aPS, apparently reduced the possibility of forming the less stable α form in the sPS crystals.

Keywords: Syndiotactic polystyrene blend; Crystallization; Polymorphism

1. Introduction

Syndiotactic polystyrene (sPS) has received extensive interest since its synthesis [1]. Many investigations have characterized its complex polymorphic crystal structure [2–7]. Depending on the thermal treatments, four major crystalline forms (termed α, β, γ and δ) can be obtained. The α and β forms both possess a planar zigzag backbone conformation, and are confirmed as the predominant polymorphs encountered under normal crystallization conditions. Investigators have identified the α form as having a hexagonal [2,3] or rhombohedral [4] structure, whereas the β form packs in an orthorhombic [5] structure. The γ and δ forms consist of the same monoclinic structure with both possessing a helical chain conformation [6,7]. The γ and δ forms can only be obtained through solvent (e.g. dichloromethane and chloroform) induced crystallization. Other mesomorphic phases have also been reported [8,9].

The crystallization kinetics and melting behavior of sPS have also been investigated [10–20]. For instance, Cimmino et al. [10] noted that at the same undercoolings, the spherulite growth rate of sPS is more than one order of magnitude higher than that of isotactic polystyrene (iPS). The equilibrium melting temperature was determined, using the extrapolation method, to be 275 °C. Hong et al. [16] observed that neat sPS shows three melting endotherms after isothermal crystallization treatments. It was suggested that the lowest and the middle melting endotherms are attributed to the meltings of β and α form crystals, respectively; the highest melting endotherm arises from the melting of recrystallized crystals. Woo et al. [17–19] investigated in more detail the relationships between the polymorphic crystals and the resulting multiple melting peaks in sPS. For the bulk crystallization of sPS, Guerra et al. [20] reported that the polymorph (α or β or mixture forms) of the crystals formed depends strongly on factors such as its thermal history including the pre-melting temperature, pre-melting time, as well the cooling rate and crystallization temperature.

* Corresponding author. Tel.: +886-3-3283016x5297; fax: +886-3-3961749.

E-mail address: maxson@mail.cgu.edu.tw (F.C. Chiu).

0032-3861/01/$ - see front matter
PII: S0032-3861(02)00349-X

Because of its excellent properties, sPS has been widely viewed as an emerging class of engineering thermoplastics. The sPS-based blends and compounds have been manufactured and investigated. The main reasons were to extend its versatility and to overcome its inherent drawbacks, such as its relatively fast crystallization rate and brittleness. The blends investigated include the miscible sPS/atactic PS (aPS) system [17,21–23], sPS/poly(2,6-dimethylphenylene oxide) (PPO) system [16,17,24,25] and the phase separated sPS/poly(vinyl methyl ether) (PVME) system [25–27]. The crystallization, melting behavior and crystalline polymorph of sPS were found to be influenced by the incorporation of the respective polymer. For example, Guerra et al. [24] concluded that the addition of PPO but aPS would be favorable for the formation of the β polymorph in the sPS crystals. Cimmino et al. [25] reported that the spherulite growth rate of sPS decreases if PPO is added, whereas it increases with the addition of PVME. On the other hand, the overall crystallization rate of sPS decreases with the addition of either PPO or PVME.

This work further investigates the sPS/aPS-50/50 (wt%) blends with three different aPS molecular weights. The effect of the aPS molecular weight on the thermal properties (e.g. glass transition temperature (T_g), crystallization and melting behavior) and the resulting crystal structure of sPS in the blends are reported here.

2. Experimental

2.1. Materials and blends preparation

Neat sPS resin manufactured by Idemitsu Kosan Co. Ltd, Japan was used in this study. The weight average molecular weight, determined by GPC, is 3.56×10^5 g mol^{-1}. Three aPSs with different molecular weights were used to mix with sPS. They were purchased from Polysciences Inc. with the weight average molecular weights around 3×10^3 g mol^{-1} (designated as aPS(L)), 5×10^4 g mol^{-1} (designated as aPS(M)), and 2×10^5 g mol^{-1} (designated as aPS(H)), respectively. These blends were prepared using the solution mixing procedure. This procedure involved dissolving equal weights of sPS and aPS in 1,2,4-trichlorobenzene (TCB) to form solutions of 3 wt% at around 130 °C. The solutions were then cast onto stainless dishes that were kept at 200 °C to rapidly evaporate the TCB solvent. To ensure complete solvent evaporation, the blends were exposed to a vacuum oven at 150 °C for at least 24 h before characterization. For comparative purposes, the sPS and aPSs parent polymers were also TCB solvent treated.

2.2. Differential scanning calorimetry (DSC)

The T_gs, crystallization kinetics and the resulting melting behavior of pure parent polymers and blends were investigated using a Perkin Elmer DSC 7 analyzer equipped with an intra-cooler. The heat flow and temperature of DSC were calibrated with standard materials, indium and zinc. Nitrogen gas was consistently purged into the DSC during the scans to prevent specimens from thermal degradation at high temperatures. For T_g determination, the parent sPS and its blends (ca. 5 mg) were melted at 340 °C for 2 min, and then quenched with ice water to obtain amorphous specimens. The amorphous specimens were further heated at a rate of 20 °C/min to determine the T_gs at the 50% thermogram transitions. Non-isothermal and isothermal crystallization experiments were conducted. The specimens were first melted at 340 °C. For the non-isothermal crystallization experiments, the specimens were cooled to room temperature at various rates (e.g. 5, 10, 20, 30 and 40 °C/min). For the isothermal crystallization experiments, the specimens were quickly cooled to various pre-set temperatures (T_cs). The crystallized specimens were subsequently heated at 20 °C/min for the corresponding melting behavior investigations.

2.3. Polarized light microscopy

Polarized light microscopy (PLM) was used to measure the isothermal crystal growth rate of sPS with or without the aPSs incorporation. An Olympus BH-2 PLM with an attached CCD camera was employed in conjunction with a Linkam THMS 600 hot stage for these studies. The temperature of the hot stage was calibrated with benzoic acid ($T_m = 122.5$ °C). The thin-film sPS and sPS/aPS specimens were prepared by casting the specimen-contained TCB solution onto glass slides. Keeping the specimens at 200 °C for 10 min under vacuum condition ensured complete solvent evaporation. The specimens were thus thermally treated, on the hot stage, like those employed in the DSC experiments to measure the crystal growth rate at selected T_cs.

2.4. Wide angle X-ray diffraction analysis

The wide-angle X-ray diffraction (WAXD) patterns of the specimens were recorded at room temperature using a Siemens D5005 X-ray unit. The X-ray used was Ni filtered Cu K_α radiation with a wavelength of 0.154 nm. The flat film technique was employed and the 2θ scan ranged from 2 to 40°. For direct comparison, the specimens were thermally treated as those for DSC experiments. The content of the α form crystal in the specimens was quantitatively estimated via the following relation [20]:

$$P_\alpha(\%) = \frac{1.8A(11.6)/A(12.2)}{1 + 1.8A(11.6)/A(12.2)} 100\% \quad (1)$$

where 1.8 is the ratio between the intensities of the 2θ diffraction peak located at 11.6 and 12.2°, respectively, for specimens with the same thickness and crystallinity in the

pure α and β forms. Meanwhile, $A(11.6)$ and $A(12.2)$ are the areas of the 2θ diffraction peaks located at 11.6 and 12.2°.

3. Results and discussion

3.1. Glass transition temperatures (T_gs) of Parent Polymers and Blends

The miscibility of the blends can be discussed in terms of the presence of single T_g. The T_gs of the amorphous parent polymers determined based on the DSC experiments are listed in Table 1. Their T_g values differ and follow the sequence of aPS(H) > sPS > aPS(M) > aPS(L). In Fig. 1 the DSC heating thermograms of the 50/50 blends (i.e. sPS/aPS(H), sPS/aPS(M) and sPS/aPS(L)) are illustrated. The single T_g located between the T_gs of the parent polymers for each blend is observed. It is thus concluded that the sPS/aPS blends investigated are miscible in the amorphous state regardless of the aPS molecular weight. The T_g values of the blends are also listed in Table 1. Included in the table are the values predicted by the Fox equation [28] and the additivity rule as well:

$$\text{Fox equation}: \quad 1/T_g = W_1/T_{g1} + W_2/T_{g2} \tag{2}$$

$$\text{additivity rule}: \quad T_g = W_1 T_{g1} + W_2 T_{g2} \tag{3}$$

where 1 and 2 represent the parent polymers and W_i is the weight fraction of parent polymer i. Evidently, the T_g values of the blends fit quite well both the Fox equation and the additivity rule (within ±3 °C of deviation).

3.2. Crystallization behavior

Fig. 2(a) and (b) shows the DSC cooling thermograms of pure sPS and its blends from the melt at a rate of 40 and 5 °C/min, respectively. Three observations can be made from these figures. First, adding the non-crystallizable aPS into the sPS depresses the crystallization onset temperature (T_o) and crystallization peak temperature (T_p, temperature at the exotherm minimum) of the sPS. Second, lowering the molecular weight of aPS also shifts the T_o and T_p of the blends to lower temperatures. Third, adding the aPS broadens the width of the sPS crystallization exotherm. Similar behaviors are also observed at other cooling rates.

Table 1
T_gs of parent polymers and their blends

Sample	DSC[a], T_g (°C)	Fox eq. T_g (°C)	Additivity rule T_g (°C)
SPS	93.8	–	–
aPS(H)	105.1	–	–
aPS(M)	70.2	–	–
aPS(L)	66.2	–	–
sPS/aPS(H)	96.8	99.4	99.5
sPS/aPS(M)	83.3	81.6	82.0
sPS/aPS(L)	78.5	79.4	80.1

[a] Experimental value.

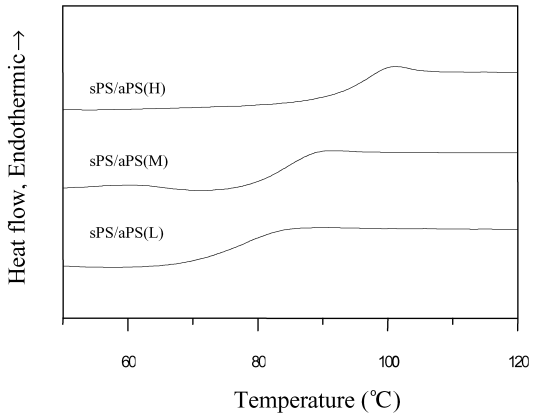

Fig. 1. DSC heating thermograms of amorphous sPS/aPS blends.

Higher cooling rates cause declines in T_o and T_p. These observations can be explained by taking into consideration of the reduction in the nucleation ability of sPS in the presence of aPSs. A similar phenomenon was reported in the iPS/PVME blend system [29]. The aPS dilution effect in the blends accounts mainly for these observations (see

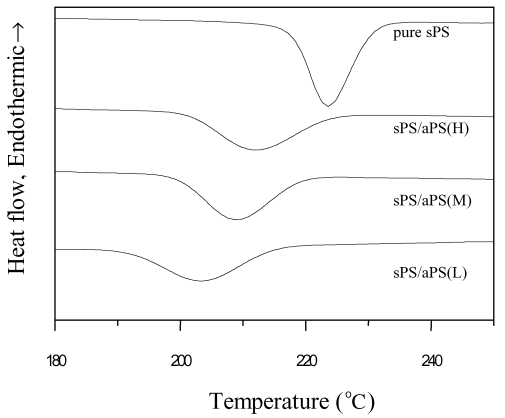

(a)

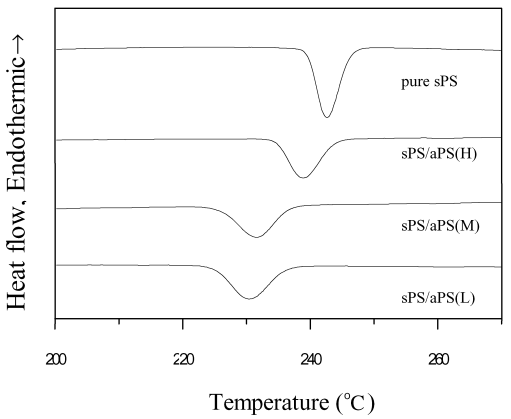

(b)

Fig. 2. DSC cooling thermograms of sPS and its blends from the melt under the rates of: (a) 40 °C/min and (b) 5 °C/min.

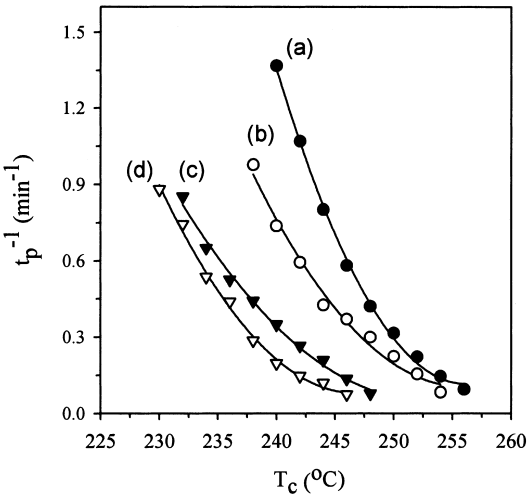

Fig. 3. t_p^{-1} as a function of T_c for (a) pure sPS; (b) sPS/aPS(H); (c) sPS/aPS(M) and (d) sPS/aPS(L).

discussion below). Moreover, the depression in the sPS crystallization temperature in the blends also suggests the presence of miscibility between these two components.

The overall kinetics of isothermal crystallization was studied by monitoring the heat evolved during the crystallization process at distinct T_cs as a function of time. The crystallization peak time (t_p) was defined as the time when the crystallization minimum occurred. Fig. 3 shows the reciprocal value of t_p (i.e. t_p^{-1}) versus T_c for the pure parent sPS and its blends. Since t_p^{-1} is recognized to be proportional to the overall crystallization rate, the results clearly indicate two features. First, as anticipated by the nucleation-controlled crystal growth theory, the crystallization rate decreases with T_c for each sample. Second, at the same T_c, the pure sPS crystallizes the fastest (the highest t_p^{-1} value), followed by the blends incorporated with aPS(H) and aPS(M). The sPS/aPS(L) blend shows the slowest overall crystallization rate at an identical T_c. This second feature corresponds well to the results obtained in the non-isothermal crystallization study (Fig. 2(a) and (b)). Additionally, the spherulite (supermolecular structure) growth rates of the samples at various T_cs were measured from the slope of the radius of growing spherulites versus time through PLM. Fig. 4 shows the typical spherulite micrographs of the sPS/aPS(H) blend grown at 248 °C. The linear growth rate, G, versus T_c for the pure sPS and its blends are plotted in Fig. 5. A trend similar to that for the overall crystallization rate result (as shown in Fig. 3) was observed. The addition of aPS decreases the spherulite growth rate of sPS at the same T_c. Furthermore, this influence is more evident as the molecular weight of aPS decreases. The effect of a non-crystallizable miscible component on the crystal growth rate of the crystalline counterpart in the blends has been studied [30,31]. In our case, two possibilities should account for this observation. The first possibility is that the higher molecular weight aPS may not be fully miscible with sPS. Therefore, the

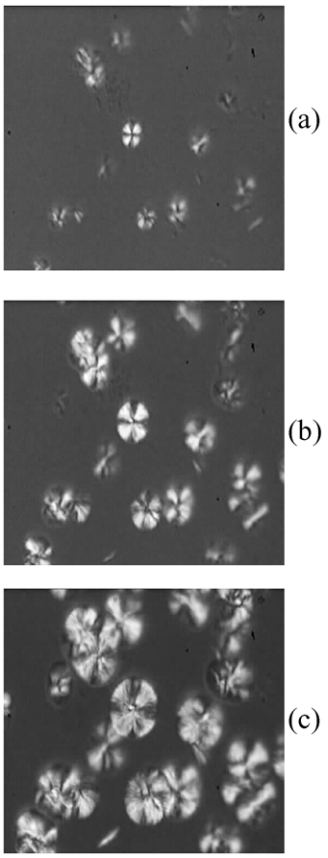

Fig. 4. Representative PLM micrographs of sPS spherulites grown at T_c = 248 °C at consecutive times ((a)–(c)) in the sPS/aPS(H) blend.

molecular segregation (expelling) of the higher molecular weight aPS during the crystallization of sPS in the blend is less hindered compared with that of the lower molecular weight aPS. This occurrence thus causes a relatively faster crystal growth rate of sPS in the blend with a higher molecular weight aPS. The second possibility is that the aPSs function as a 'diluent' in the blends, which leads to a

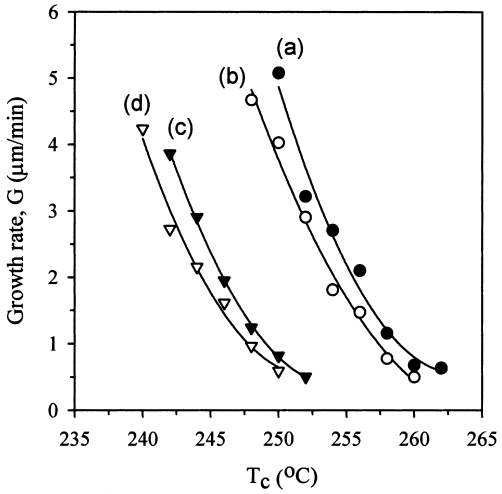

Fig. 5. Crystal growth rate (G) vs. T_c for (a) pure sPS; (b) sPS/aPS(H); (c) sPS/aPS(M) and (d) sPS/aPS(L).

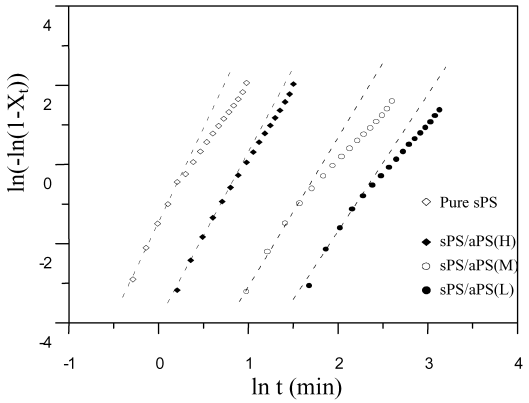

Fig. 6. Avrami plots of sPS and its blends at $T_c = 244$ °C.

decrease in the equilibrium melting temperature (T_m^0) of sPS. The 'diluent' effect is more evident with the lower molecular weight aPS (see Section 3.3). Therefore, if the samples are crystallized at the same T_c, the order of the undercooling (ΔT) for the samples will be sPS > sPS/aPS(H) > sPS/aPS(M) > sPS/aPS(S). The crystal growth rate will thus be expected to be sPS > sPS/aPS(H) > sPS/aPS(M) > sPS/aPS(S) at the same T_c. Nevertheless, the first possibility may be ruled out since the DSC experiments have proved the miscibility between the sPS and aPS regardless of aPS molecular weight. Accordingly, it can be concluded that the second possibility—'diluent effect' accounts for this observation.

The well-known Avrami equation [32–34] was used to analyze the overall crystallization kinetics obtained from the DSC experiments:

$$1 - X_t = \exp(-Kt^n) \tag{4}$$

which is always cast into

$$\ln[-\ln(1 - X_t)] = \ln K + n \ln t \tag{5}$$

where X_t is the fractional crystallinity at time t, n is the Avrami exponent and K is the kinetic constant. As is widely recognized, the Avrami exponent n can provide qualitative information on the nature of the nucleation and crystal growth geometry. Fig. 6 shows the representative Avrami plots for the samples at $T_c = 244$ °C. The experimental data fits the Avrami equation at short crystallization time (low crystallinity region), which indicates secondary crystallization is present for pure sPS and its blends as well. The Avrami exponents determined from the slopes of the plots for all of the samples at various T_cs are mostly non-integral, and range from 3.4 to 4.7 with slightly lower values for these blends. These values suggest that a mixed nucleation mechanism (thermal and athermal) is involved regardless of the addition and molecular weight of aPS.

3.3. Melting behavior

Fig. 7(a) and (b) shows the DSC heating thermograms of the samples cooled from the melt with a rate of 5 and 40 °C/min, respectively. Note that for each sample pre-cooled at 5 °C/min exhibits double melting peaks (Fig. 7(a)), whereas a pre-cooling rate of 40 °C/min causes one major melting peak with an ex-minor exothermic shallow (Fig. 7(b)). This phenomenon is ascribed primarily to the melting–recrystallization–remelting process of sPS crystals (the β form, see Section 3.4) during the heating scans [13,16,19]. That is, a pre-cooling rate of 40 °C results in a profound recrystallization process during the subsequent heating, thus a large remelting peak occurs. On the other hand, a pre-cooling rate of 5 °C/min results in a fractional recrystallization process followed by a relatively smaller remelting peak. Another important feature in this figure is that the sPS in general shows lower melting temperatures in the blends compared with those in the pure state. Moreover, the lower the molecular weight of the aPS in the blends, the lower the sPS melting temperatures. As stated previously, this suggests the miscibility of these blends though the crystals formed are not in a real equilibrium state.

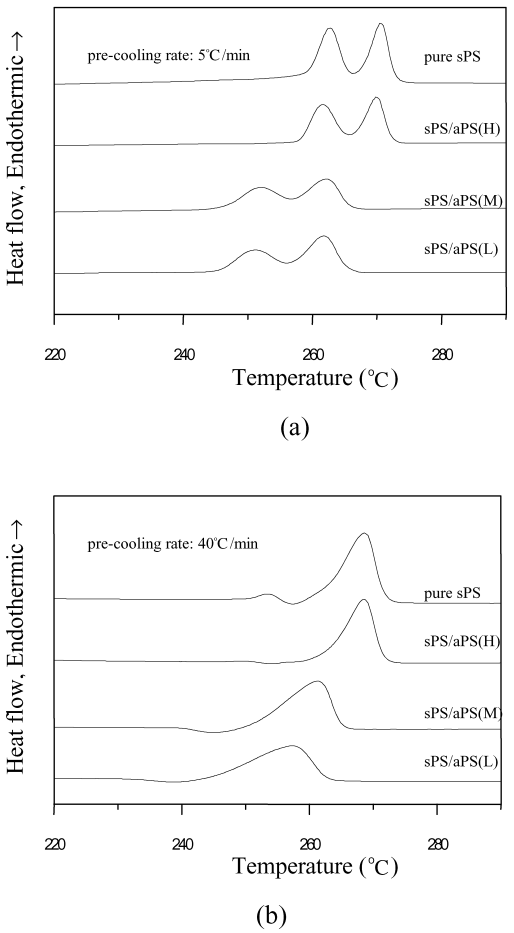

Fig. 7. DSC melting traces of sPS and its blends cooled from the melt with the rates of: (a) 5 °C/min and (b) 40 °C/min.

The DSC melting behavior of the samples isothermally crystallized at various T_cs are shown in Fig. 8(a)–(d). Three common features are observed in these figures. First, two distinct melting peaks are evident at low T_cs (except for the

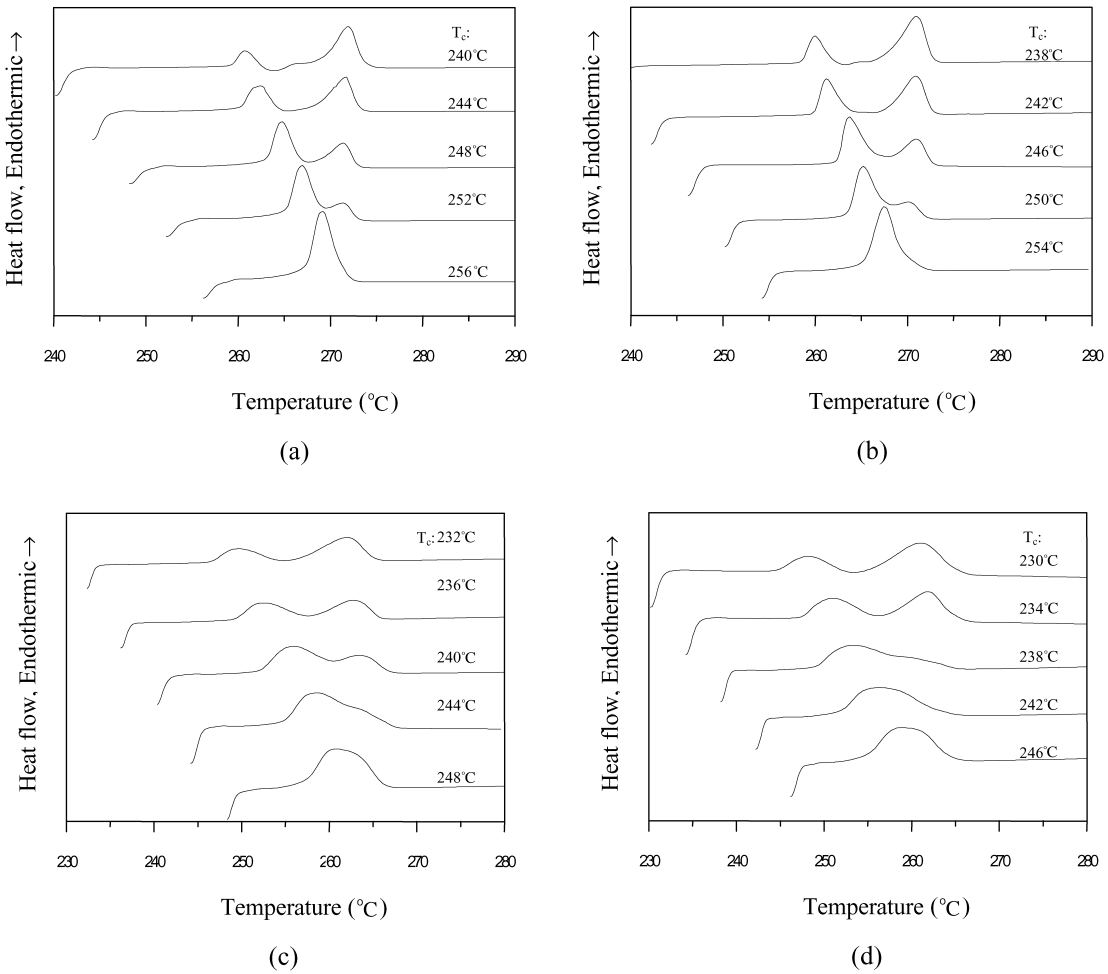

Fig. 8. DSC melting traces of sPS and its blends isothermally crystallized at indicated T_cs: (a) pure sPS; (b) sPS/aPS(H); (c) sPS/aPS(M) and (d) sPS/aPS(L).

existence of a hardly detectable peak located between the two main peaks for the $T_c = 240$ °C curve of pure sPS, and $T_c = 238$ °C curve of sPS/aPS(H) blend), which becomes one dominant melting peak as T_c increases. Second, the low-melting peak (peak I) shifts to a higher temperature with T_c, but the high-melting peak (peak II) stays nearly constant with T_c. Third, the intensity ratio between peak I and peak II increases with T_c. From the crystal structure identification in the following section, the crystals formed are mixtures of α and β forms at low T_cs, and is basically the β form at high T_cs. All of the earlier observations indicate that the melting–recrystallization–remelting phenomenon exists not only for isothermally crystallized pure sPS but also for its blends with aPS. Because a higher T_c results in a more perfect crystal, the recrystallization phenomenon declines as T_c increases (resulting in one dominant melting peak). The peak I and peak II shift to lower temperatures with the addition of aPSs, and this phenomenon becomes more evident with aPS having a lower molecular weight. Table 2 lists the estimated peak I and peak II values. The ratio between the peak I and peak II areas represents the degree of melting–recrystallization–remelting occurring during the heating scans. A higher ratio means a lower degree of melting–recrystallization–remelting. Fig. 9 shows the peak area ratio as a function of T_c for each sample. The combined effect of T_c and adding aPS on the melting–recrystallization–remelting of sPS crystals is revealed. The melting–recrystallization–remelting phenomenon is more evident for pure sPS compared with its blends at the same T_c.

Table 2
Low-melting temperature ($T_{m,1}$) and high-melting temperature ($T_{m,2}$) of isothermally crystallized sPS and its blends

Sample	T_c (°C)	$T_{m,1}$ (°C)	$T_{m,2}$ (°C)	Sample	T_c (°C)	$T_{m,1}$ (°C)	$T_{m,2}$ (°C)
sPS	240	260.4	271.4	sPS/aPS(H)	238	259.7	271.1
	244	261.7	271.0		242	261.0	270.8
	248	264.7	270.8		246	263.7	271.0
	252	266.9	270.9		250	265.2	270.6
	256	269.1	Absent		254	267.5	Absent
sPS/aPS(M)	232	249.6	262.0	sPS/aPS(L)	230	248.2	261.0
	236	252.3	262.3		234	250.9	261.4
	240	255.9	263.3		238	253.4	261.2
	244	258.6	263.5		242	256.2	Absent
	248	260.8	Absent		246	258.9	Absent

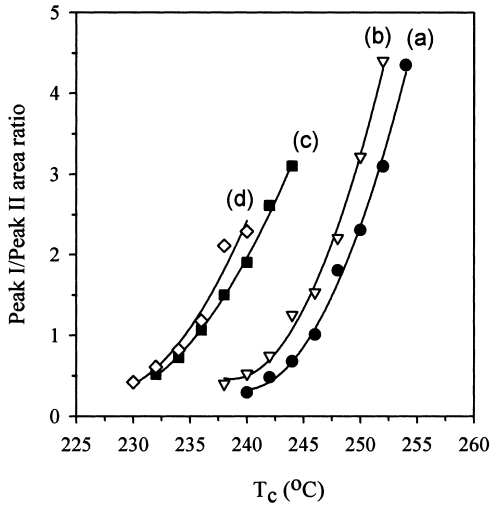

Fig. 9. Ratio of peak I/peak II area as a function of T_c for (a) pure sPS; (b) sPS/aPS(H); (c) sPS/aPS(M) and (d) sPS/aPS(L).

Moreover, this phenomenon declines as the molecular weight of aPS declines. Fig. 10 shows the peak area ratio vs. t_p^{-1} for each sample. It is interesting to note that all of the data points fall nearly onto a master curve. This result implies that the degree of melting–recrystallization–remelting of sPS crystals is dependent primarily on the pre-overall crystallization rate instead of the existence of aPS. That is when pure sPS and its blends are crystallized at distinct T_cs but with the same t_p^{-1} value, the peak area ratio is nearly identical for each sample. This observation suggests that adding aPS does not affect the stability of the β form crystals (see Section 3.4) formed, if the overall crystallization rate of sPS itself is kept constant.

3.4. Crystal structure

Fig. 11 shows the WAXD spectra of pure sPS and its blends crystallized from the melt at a cooling rate of 20 °C/min. As mentioned in Section 2, the intensities of the

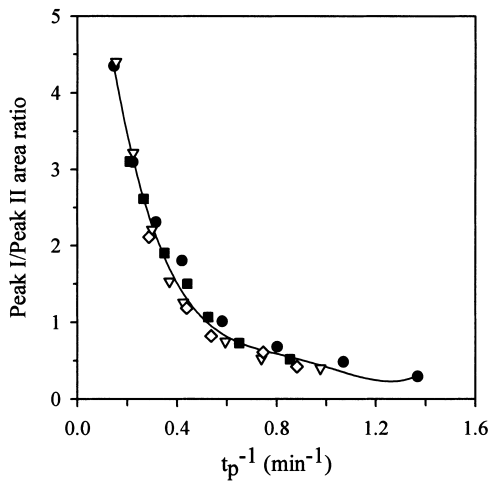

Fig. 10. Ratio of peak I/peak II area as a function of t_p^{-1} for sPS and its blends. (symbols as in Fig. 9).

Table 3
The percentage content of α form crystals in pure sPS and in its blends under different crystallization conditions

Crystallization condition	P_α (%)			
	sPS	sPS/aPS(H)	sPS/aPS(M)	sPS/aPS(L)
Cooled-20[a]	75.2	11.5	<5	<5
Cooled-air[a]	90.6	81.6	70.3	59.5
Iso-240 °C[a]	84.6	55.1	<5	<5
Iso-250 °C[a]	48.1	21.3	<5	<5

[a] Cooled-20: cooling rate = 20 °C/min; cooled-air: air-quenched; iso-240 °C: T_c = 240 °C; iso-250 °C: T_c = 250 °C.

diffraction peaks located at $2\theta = 11.6$ and 12.2° were employed to estimate the α form content in the crystals. Both diffraction peaks appear for the pure sPS indicating that the crystals formed are mixtures of the α form and β form. Only one diffraction peak ($2\theta = 12.2°$) is shown for the blends except for a very minor $2\theta = 11.6°$ peak existing for the sPS/aPS(H) blend. The percentage content of α form in the crystals formed under a cooling rate of 20 °C/min and that of air-quenched samples owing to Eq. (1) are listed in Table 3. Adding aPS reduces the possibility of forming the α form sPS crystals is evident; and this influence is more evident with lower molecular weight aPS. The fact that a faster cooling rate results in a higher α form crystal content has been reported before [13,20]. Fig. 12 shows the representative WAXD spectra of samples isothermally crystallized at 240 °C. The intensity of the diffraction peak at $2\theta = 12.2°$ compared to that of $2\theta = 11.6°$ increases with the addition of aPS, and moreover with lower molecular weight aPS. A similar trend was noted at other T_cs. The calculated P_α values for the samples crystallized at T_c = 240 and 250 °C are also listed in Table 3. A higher T_c produces a more stable β form crystal. Comparing the WAXD results with the DSC melting thermograms results infers that the DSC main melting peaks correspond to the β form crystals. From the above crystal structure analysis, we can conclude that under the same crystallization conditions,

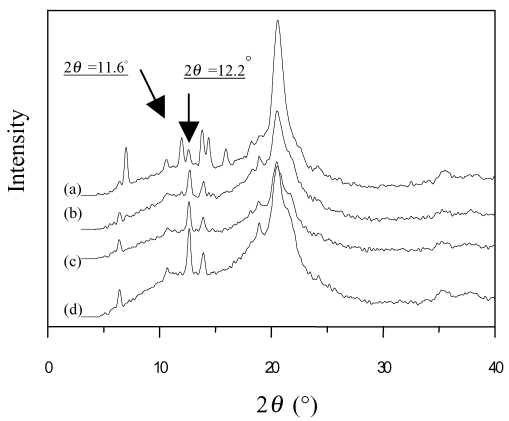

Fig. 11. WAXD spectra of sPS and its blends crystallized at a rate of 20 °C/min from the melt. ((a), (b), (c) and (d) as in Fig. 9).

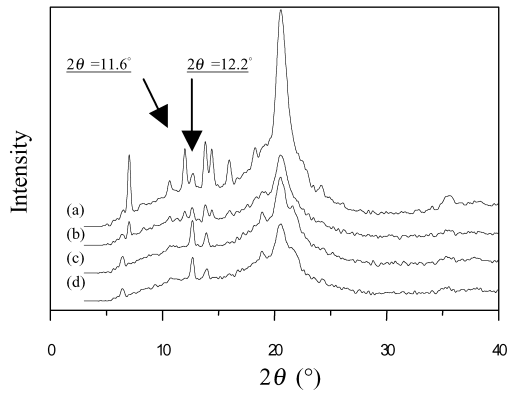

Fig. 12. WAXD spectra of sPS and its blends isothermally crystallized at $T_c = 240$ °C from the melt. ((a), (b), (c) and (d) as in Fig. 9).

aPS will prevent (fully or partly) the formation of the less stable α form sPS crystals, especially for aPS with a lower molecular weight. However, the reason why aPS exhibits such an effect is not clear at this moment. Supplementary experiments are being conducted to explain this observation.

4. Conclusions

This study compared the thermal properties and the crystal structure of sPS and its blends with different molecular weight aPS. The single T_g of each blend was observed, which implied the miscibility of the blends. From the overall melt crystallization data and the linear crystal growth rates, we could infer that (at the same T_c) the lower the molecular weight of the incorporated aPS, the slower the nucleation and crystal growth of sPS. Avrami analysis revealed that the nucleation process of pure sPS and its blends was comparable and the crystal growth geometry was three-dimensional. Multiple DSC melting endotherms were observed for isothermally and non-isothermally crystallized pure sPS and its blends. These DSC melting endotherms were T_c dependent. The low- and high-melting-temperature peaks were ascribed mainly to the meltings of the originally formed and the recrystallized (during heating scans) β form crystals. The barely observed middle-melting-temperature peak was associated with the α form crystals. Furthermore, the blends showed lower melting temperatures than those of pure sPS. The lower the molecular weight of aPS, the lower the melting temperatures that the blends possessed. The melting–recrystallization process of sPS during heating scans was dependent primarily on the pre-crystallization rate of sPS, regardless of the incorporation of aPS. The percentage content of α form sPS crystals formed under different conditions was quantitatively determined and increased with an increasing cooling rate and decreasing T_c. Interestingly, the incorporation of aPS into sPS declined the α form crystal content and this was more evident as the molecular weight of aPS decreased.

Acknowledgments

The authors would like to thank the National Science Council of the Republic of China for financially supporting this research under Contract No. NSC90-2216-E-182-003.

References

[1] Ishihara N, Seimiya T, Kuramoro M, Uoi M. Macromolecules 1986; 19:2464.
[2] Greis O, Xu Y, Asano T, Peterman J. Polymer 1989;30:590.
[3] Sun Z, Miller RL. Polymer 1993;34:1963.
[4] De Rosa C, Guerra G, Petraccone V, Corradini P. Polym J 1991;23: 1435.
[5] De Rosa C, Rapacciuolo G, Guerra G, Petraccone V, Corradini P. Polymer 1992;33:1423.
[6] Chanati Y, Shimane Y, Inagaki T, Ijitsu T, Yukinari T, Shikuma H. Polymer 1993;34:1620.
[7] Chanati Y, Shimane Y, Inoue Y, Inagaki T, Ishioka T, Ijitsu T, Yukinari T. Polymer 1992;33:488.
[8] De Candia F, Ruvolo Filho A, Vittoria V. Colloid Polym Sci 1991; 269:650.
[9] De Candia F, Guadagno L, Vittoria V. J Macromol Sci, Phys B 1995; 34(3):273.
[10] Cimmino S, Di Pace E, Martuscelli E, Silvestre C. Polymer 1991;32: 1080.
[11] Wesson RD. Polym Engng Sci 1994;34:1157.
[12] St Lawrence S, Shinozaki DM. Polym Engng Sci 1997;37:1825.
[13] Chiu FC, Peng CG, Fu Q. Polym Engng Sci 2000;40:2397.
[14] Chiu FC, Shen KY, Tsai SHY, Chen CM. Polym Engng Sci 2001;41: 881.
[15] Wu HD, Wu ID, Chang FC. Macromolecules 2000;33:8915.
[16] Hong BK, Jo WH, Lee SC, Kim J. Polymer 1998;39:1793.
[17] Woo EM, Wu FS. Macromol Chem Phys 1998;199:2041.
[18] Sun YS, Woo EM. Macromolecules 1999;32:7836.
[19] Woo EM, Sun YS, Yang CP. Prog Polym Sci 2001;26:945.
[20] Guerra G, Vitagliano VM, De Rosa C, Petraccone V, Corradini P. Macromolecules 1990;23:1539.
[21] Hong BK, Jo WH, Kim J. Polymer 1998;39:3753.
[22] Bonnet M, Buhk M, Trogner G, Rogausch KD, Petermann J. Acta Polym 1998;49:174.
[23] Wu FS, Woo EM. Polym Engng Sci 1999;39:825.
[24] Guerra G, De Rosa C, Vitagliano VM, Petraccone V, Corradini P. J Polym Sci, Polym Phys 1991;29:265.
[25] Cimmino S, Di Pace E, Martuscelli E, Silvestre C. Polymer 1993;34: 2799.
[26] Cimmino S, Di Pace E, Martuscelli E, Silvestre C. Polymer 1991;32: 251.
[27] Cimmino S, Di Pace E, Martuscelli E, Silvestre C, Rice DM, Karasz FE. Polymer 1993;34:214.
[28] Fox TG. Bull Am Phys Soc 1956;1:123.
[29] Amelino L, Martuscelli E, Sellitti C, Silvestre C. Polymer 1990;31: 1051.
[30] Wang TT, Nishi T. Macromolecules 1977;10:421.
[31] Alfonso GC, Russell TP. Macromolecules 1986;19:1143.
[32] Avrami M. J Chem Phys 1939;7:1103.
[33] Avrami M. J Chem Phys 1940;8:212.
[34] Avrami M. J Chem Phys 1941;9:177.